ISSN 1063-7397, Russian Microelectronics, 2020, Vol. 49, No. 1, pp. 16–24. © Pleiades Publishing, Ltd., 2020.
Russian Text © The Author(s), 2020, published in Mikroelektronika, 2020, Vol. 49, No. 1, pp. 18–26.

Arrays of Carbon Nanotubes in a Field of Continuous Laser Radiation

S. A. Afanas'ev[a, *], I. O. Zolotovsky[a, c], A. S. Kadochkin[a, c], S. G. Moiseev[a, c], V. V. Svetukhin[b], A. A. Pavlov[c] and S. V. Bulyarsky[c]

[a] *Ulyanovsk State University, National Educational Center of Silicon–Carbon Nanotechnology, Ulyanovsk, 432017 Russia*
[b] *Scientific and Production Complex Technological Center, Zelenograd, Moscow, 124498 Russia*
[c] *Institute of Nanotechnologies of Microelectronics, Russian Academy of Sciences, Moscow, 119991 Russia*
**e-mail: asa_rpe@mail.ru*

Received May 27, 2019; revised July 26, 2019; accepted July 26, 2019

Abstract—A numerical analysis of the phase-matching conditions during the incidence of one or two counterpropagating laser beams on an ordered array of single-walled carbon nanotubes (CNTs) is performed. The conditions for the generation of slow surface plasmon waves of the terahertz (THz) and far infrared range propagating along the nanotubes of the irradiated array are determined. It is shown that the plasmon frequency can be controlled by changing the angle of incidence of laser radiation on the structure under study. Thus, it is possible to fulfill the condition of longitudinal resonance, in which each array nanotube is a dipole antenna radiating at the plasmon frequency. In this case, the array forms a system of a large number of in-phase emitters, which allows increasing the efficiency of conversion of laser radiation into THz radiation in comparison with a single nanoantenna.

DOI: 10.1134/S1063739720010023

INTRODUCTION

Currently, the development of compact terahertz (THz) radiation generators operating at room temperature is an urgent task. Such generators could find practical applications in spectroscopy, safety systems, medical diagnostics, and other fields of science and technology [1, 2].

In modern solid state THz radiation sources, parametric interaction of a laser pulse with a semiconductor structure is usually carried out [1–5]. Semiconductor quantum cascade lasers in the THz range operate only at cryogenic temperatures and do not possess the possibility of significant frequency tuning. Gas lasers, although they operate at room temperature, are also not able to significantly tune the radiation wavelength. THz radiation sources created on the basis of femtosecond lasers have an extremely wide emission spectrum (of the order of 1 THz), as a result of which only a small part of the energy is converted to THz radiation, usually the conversion efficiency does not exceed 10^{-3} [3–5].

It is possible to increase the conversion efficiency of laser radiation into THz by going on to conversion in a continuous mode. Also, to increase the efficiency, the target may contain various plasmon structures. One of the promising directions for creating THz generators is the use of arrays of carbon nanotubes (CNTs) and nanocomposites based on them, irradiated with continuous laser radiation. The combination of a large number of unique properties of CNTs in combination with their geometric dimensions makes them promising when considering the generation of THz (and microwave) radiation [6–16]. The proposed applications of CNTs as emitters of electromagnetic waves are based on the fact that CNTs can act as a transmission line (waveguide) supporting the propagation of a surface electromagnetic wave [7, 11–13, 17–22]. An important feature of generating a submillimeter wave array of CNTs is the need for significant (by a factor of over 100) deceleration of the surface waves compared with the speed of light in a vacuum.

In this paper, we consider the generation mechanism under the influence of laser radiation of slow surface plasmon polaritons (PPs) in arrays of single-walled CNTs. Plasmon waves generated in a CNT array by one or two laser beams can be considered as antennas providing the generation of radiation in the submillimeter range. The conditions for the generation of PPs in similar structures are obtained using laser radiation at a wavelength of 1.06 μm, which employs the most common and affordable fiber and solid-state laser sources with high average and peak powers.

Two generation schemes will be considered in this work.

(1) The use of an array of two laser sources with slightly different frequencies for exciting slow PPs in

Abbreviations: CNT—carbon nanotube; PP—plasmon polaritons; THz—terahertz.

CNTs. In this case, the corresponding slow PP is generated at a difference frequency.

(2) Slow PPs are excited in a CNT array under conditions of the interaction of narrow-band laser radiation (incident and diffracted waves) with periodically located CNTs. In this case, the self-decay (of the type of parametric three-photon interaction in a periodic structure) of the initial laser wave into a diffracted wave and a PP on the surface of the nanotubes is considered.

Both in the first and in the second cases, the phase-matching conditions of the corresponding wave processes should be realized.

PHASE-MATCHING CONDITIONS

We consider a two-dimensional ordered array of identical single-walled CNTs of radius a located parallel to each other (Fig. 1). A laser beam of frequency ω_1 with wave number $k_1 = \omega_1/s$ (s is the speed of light in a vacuum) falls on the structure at angle θ_1 to axis x (normal to the axis of symmetry of the tubes). The laser field will be approximated by a plane wave of TM polarization. For a given polarization of the incident wave, there is a component of its electric field directed along the axes of the tubes (axis z). Its presence is a necessary condition for the occurrence of the longitudinal component of the current density vector flowing over the surface of the tube and the excitation of a slowed-down surface wave guided by the tube acting as a waveguide [7, 11, 17–22].

In the first version, this scheme will be considered under the conditions of two-beam excitation, when the second (incoming) laser beam with a different ω_1, albeit, close to its frequency of ω_2 falls onto the CNT array at angle θ_2 (Fig. 1a). In this case, PP generation in nanotubes occurs at a the difference frequency $\Omega = \omega_1 - \omega_2$. In this case, the phase matching condition is written as

$$k_1 \sin\theta_1 - k_2 \sin\theta_2 = \beta(\Omega), \quad (1)$$

where $k_2 = \omega_2/s$, and β is the wave number of the PP excited in nanotubes. We can ensure compliance with condition (1), for example, by choosing the desired angle θ_2 at a fixed angle of incidence of the reference beam θ_1.

The second (less technically complicated) scheme can be implemented in the presence of only one laser beam (Fig. 1b); however, this requires the strict periodicity of an array of parallel CNTs. The array is in this case a diffraction grating with period d (d is the distance between adjacent nanotubes). A diffracted beam of reduced frequency $\omega_2 = \omega_1 - \Omega$ has a wave vector of magnitude $k_2 = \omega_2/s$, at angle θ_2 to axis x. The Bragg diffraction condition, taking into account the generation of PPs excited at the difference frequency Ω and propagating along the tubes (axis z) with wave vector $\boldsymbol{\beta}$ has the form

$$\mathbf{k}_1 = \mathbf{k}_2 + \boldsymbol{\beta}(\Omega) \pm \mathbf{q}, \quad (2)$$

where $\mathbf{q}$ is the wave vector of the periodic structure ($q = 2\pi p/d$, p is the order of diffraction). Further, we will take into account only diffraction beams of the first order with $p = \pm 1$.

In projections on axes x and z, the introduced coordinate system (2) will be written as

$$\begin{cases} k_1 \cos\theta_1 - k_2 \cos\theta_2 = q, \\ k_1 \sin\theta_1 - k_2 \sin\theta_2 = \beta(\Omega). \end{cases} \quad (3)$$

For a real array of CNTs, it is rather difficult to ensure the periodicity of the irradiated structure. However, in the case of an unordered but sufficiently dense array, the condition of phase synchronization will be satisfied for a certain number of tubes, the arrangement of which satisfies (3).

DISPERSION RATIO

In order to solve and analyze phase relationships (1) and (3), it is necessary to have a dispersion ratio, i.e., dependence $\beta(\Omega)$ for the PP wave vector propagating along the tubes. There are various approaches to solve the electrodynamic problem of the propagation of a surface wave in a waveguide formed by CNTs [7, 18–24]; however, but dispersion dependences obtained in this way are in close agreement with each other. In this work, we use the dispersion relation for a surface TM wave in a metal single-walled CNT without losses, given in [19]:

$$i\Omega\varepsilon_0 = \sigma_{zz}\beta^2 a I(\beta a) K(\beta a), \quad (4)$$

where ε_0 is the dielectric constant, $I(\beta a)$ and $K(\beta a)$ are modified Bessel functions of the 1st and 2nd kind, and σ_{zz} is the longitudinal component of the conductivity tensor of a metal single-walled CNT:

$$\sigma_{zz} = \frac{in_0 e^2}{m_e \Omega}, \quad (5)$$

where n_0 is the equilibrium surface density of π-electrons in CNTs, e is the elementary charge, and m_e is the effective mass of the electron.

For the relation n_0/m_e in (5), the following estimate was obtained in [25]:

$$\frac{n_0}{m_e} = \frac{2V_F}{\pi^2 \hbar a}$$

where $\hbar$ is the Planck constant and V_F is the Fermi velocity, the value of which for metal single-walled CNTs is estimated as $V_F \approx (0.9 - 1) \times 10^6$ m/s [20].

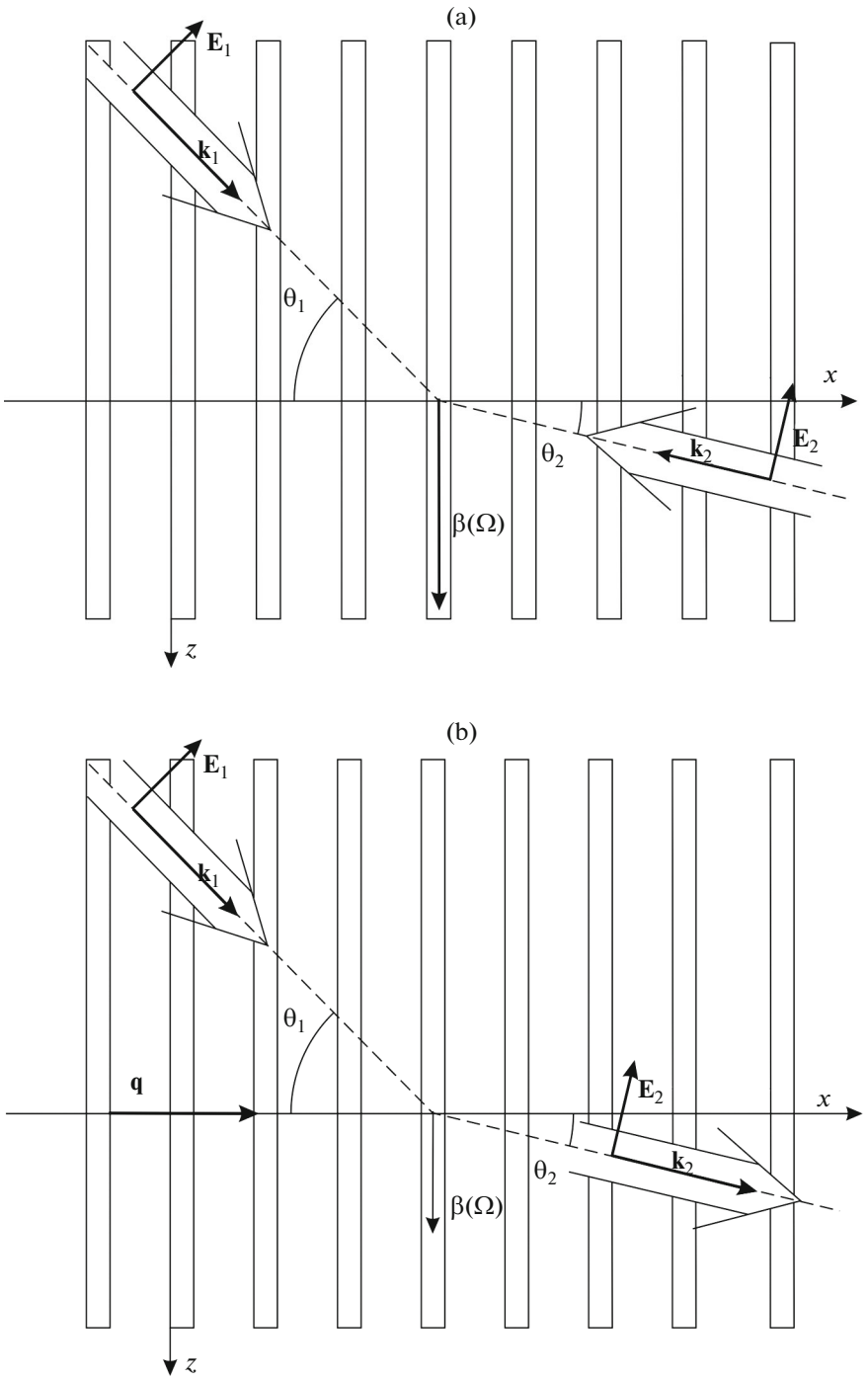

Fig. 1. Geometry of the problem: generation of PP in a CNT array upon irradiation with two (a) and one (b) laser beams.

Next, we analyze the conditions for the existence of solutions of Eqs. (1) and (3), and their numerical analysis is carried out taking into account ratio (4) for various values of the angle of incidence of the reference laser beam in the range of its values of $0° \le \theta_1 \le 90°$.

RESULTS AND DISCUSSION

A. Two-Beam Scheme

The results of the numerical analysis of condition (1) for a two-beam scheme are presented in Fig. 2, where we show the dependence of the angle of incidence θ_2

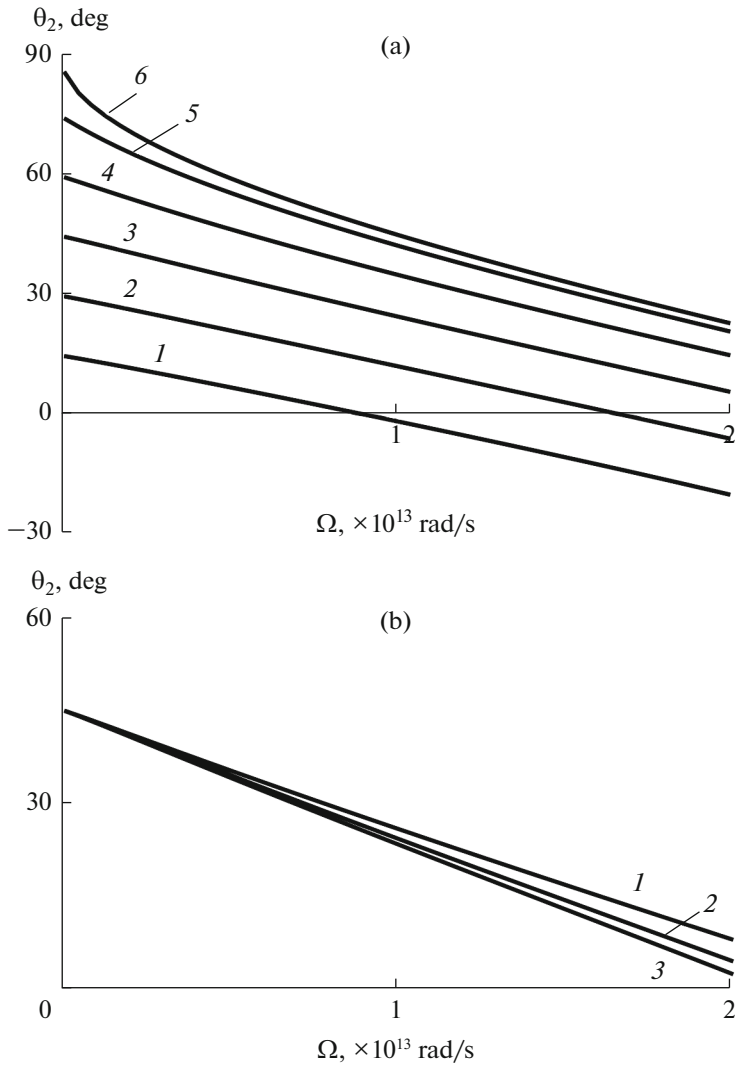

Fig. 2. Dependences of the angle of incidence of the second laser beam on the difference frequency: (a) for $a = 1$ nm, $\theta_1 = 15°$, 30°, 45°, 60°, 75° and 90° (*1*–*6*); (b) at $\theta_1 = 45°$, $a = 0.5$, 1.5, 2.5 nm (*1*–*3*).

of the second beam on frequency Ω of the PPs excited in an array of nanotubes. The calculations were carried out at fixed values of the angle of incidence θ_1, taking into account relation (4).

In Fig. 2a, the dependences $\theta_2(\Omega)$ are shown for different values of the angle of incidence θ_1 at a fixed value of the nanotube radius of $a = 1$ nm. It can be seen that angle θ_2 decreases with increasing frequency Ω and when the values of angle θ_1 are not excessively large the sign can change (the direction of reading angle θ_2 shown in Fig. 1a is considered positive). Note the linear nature of the presented dependences, which is violated only at sufficiently large angles of incidence θ_1 (starting at about 60°) for low frequencies of Ω from the studied range.

In Fig. 2b the dependences $\theta_2(\Omega)$ are given for different values of the radius of nanotube a at a fixed angle $\theta_1 = 45°$. It can be noted that value a weakly affects the course of dependence, and with a decrease in frequency Ω, its influence becomes insignificant. Thus, this scheme can be practically insensitive to possible variations in the transverse dimensions of individual nanotubes of the array.

B. Self-Decay of the Laser Beam

We will look for roots θ_2 and Ω of system (3) depending on the angle of incidence θ_1 of the laser beam on the structure at a fixed value of the lattice period d. From the first and second equations of system (3), we get the expressions for the cosine and sine of the desired angle θ_2:

$$\cos\theta_2 = \frac{k_1\cos\theta_1 \mp q}{k_2} = \frac{\omega_1\cos\theta_1 \mp qc}{\omega_1 - \Omega}, \quad (6)$$

$$\sin\theta_2 = \frac{k_1\sin\theta_1 - \beta(\Omega)}{k_2} = \frac{\omega_1\sin\theta_1 - \beta(\Omega)c}{\omega_1 - \Omega}, \quad (7)$$

from which the following relation follows:

$$(\omega_1 - \Omega)^2 = (\omega_1\cos\theta_1 \mp qc)^2 + (\omega_1\sin\theta_1 - \beta(\Omega)c)^2. \quad (8)$$

By numerically solving (8), we find Ω, and then from (6) and (7), we find angle θ_2.

Some important regularities of the laser beam's self-decay process can be obtained analytically using the approximation $\Omega \ll \omega_1$. Then Eq. (6) takes the form

$$\cos\theta_2 = \cos\theta_1 - q/k_1 = \cos\theta_1 \mp \lambda_1/d, \quad (9)$$

where λ_1 is the wavelength of incident radiation. When $q > 0$, the condition $d \geq \lambda_1/2$, bounding the the value of the grating period from below follows from (9). It is also seen that the situation with $q < 0$ is possible only with $d \geq \lambda_1$.

Now rewriting (7) in the approximation $\Omega \ll \omega_1$ as

$$\sin\theta_2 = \sin\theta_1 - \beta(\Omega)/k_1,$$

after taking (9) into consideration, we can obtain the size β of the PP's wave vector:

$$\beta/k_1 = \sin\theta_1 \pm \sqrt{1 - (\cos\theta_1 \mp \lambda_1/d)^2}. \quad (10)$$

Figure 3 shows the results of a graphical solution of Eq. (8) regarding variable Ω in several special cases for an array of nanotubes of radius $a = 1$ nm. First, consider the situation $d \geq \lambda_1$, which admits two special cases differing in the sign of parameter q. It should also be noted that relation (10) allows the possibility of two signs of the wave number β, i.e., PP propagation along the tubes in both positive and negative directions of axis z. In other words, value β changes sign at the critical value of the angle of incidence

$$\theta_1^{cr} = \arccos(\lambda_1/2d). \quad (11)$$

At $d \geq \lambda_1$, the value θ_1^{cr} lies in the range from 60° to 90°.

In Figs. 3a and 3b, the results are presented for a lattice with period $d = 1.5$ μm at various values of the angle of incidence θ_1 for cases $q > 0$ (a) and $q < 0$ (b). The solid bold line shows the frequency dependence $Y_1(\Omega)$ on the left side of Eq. (8) independently of θ_1. The thin lines correspond to dependences $Y_2(\Omega)$ on the right side, the solid lines refer to positive values β of the wave vector, and the dashed lines refer to negative values β of the wave vector. The intersection points of the thick and thin lines give the frequencies of the PPs propagating in nanotubes.

When $q > 0$ (Fig. 3a), in the range of angles $0 \leq \theta_1 < \theta_1^{cr}$, there are two roots corresponding to two PPs with different frequencies and different propagation directions (for example, curves *2* and *2'* for $\theta_1 = 30°$). For $\theta_1 = 0$, the solid curve *1* merges with the dashed *1'*, which corresponds to two PPs of the same frequency. At the critical angle of incidence $\theta_1 = \theta_1^{cr} \approx 69°$ (curves *3*, *3'*), the root corresponding to the plasmon with $\beta < 0$ disappears, and when $\theta_1 > \theta_1^{cr}$, we have two roots corresponding to the plasmons of one (positive) direction of propagation (curves *4*, *4'*).

Solutions with $q < 0$ are possible if the angle of incidence θ_1 exceeds the value

$$\theta_1^{min} = \arccos(1 - \lambda_1/d).$$

In the conditions of Fig. 3b, $\theta_1^{min} \approx 73°$; at this angle of incidence, there is only one solution (curve *3*); at $\theta_1 < \theta_1^{min}$, there are no solutions (curves *1*, *2*); and for $\theta_1 > \theta_1^{min}$ (curve *4*), there are two solutions, both of which correspond to plasmons with $\beta > 0$.

The values of angle θ_2 corresponding to the two roots of Eq. (8) (if any) differ only in sign; i.e., the directions of the two diffracted beams are symmetric about axis x. This is schematically shown in Fig. 4, where, in addition to the wave vectors of the incident and diffracted beams, wave vectors β PP generated in a CNT array are shown. Figure 4a displays the typical situation for the interval of incidence angles $\theta_1 < \theta_1^{cr} < \theta_1^{min}$, where there are two diffracted beams with wave vectors $\mathbf{k}_{21}$ and $\mathbf{k}_{22}$. For incidence angles from the interval $\theta_1 > \theta_1^{min} > \theta_1^{cr}$ (Fig. 4b), in addition to the two beams ($\mathbf{k}_{21}^+$ and $\mathbf{k}_{22}^+$) arising in the case $q > 0$, another two beams ($\mathbf{k}_{21}^-$ and $\mathbf{k}_{22}^-$) appear that satisfy the condition $q < 0$. Moreover, for $q > 0$, the minimum diffraction angle $\theta_{2\,min}^+ = \arccos(1 - \lambda_1/d)$ corresponds to the angle of incidence $\theta_1 = 0$, and the maximum $\theta_{2\,max}^+ = \arccos(-\lambda_1/d)$ is realized when $\theta_1 \to 90°$. Thus, angles θ_2^+ can be either acute or obtuse; i.e., either radiation passes through the structure or its reflection. For $q < 0$, the diffraction angle θ_2^- can only

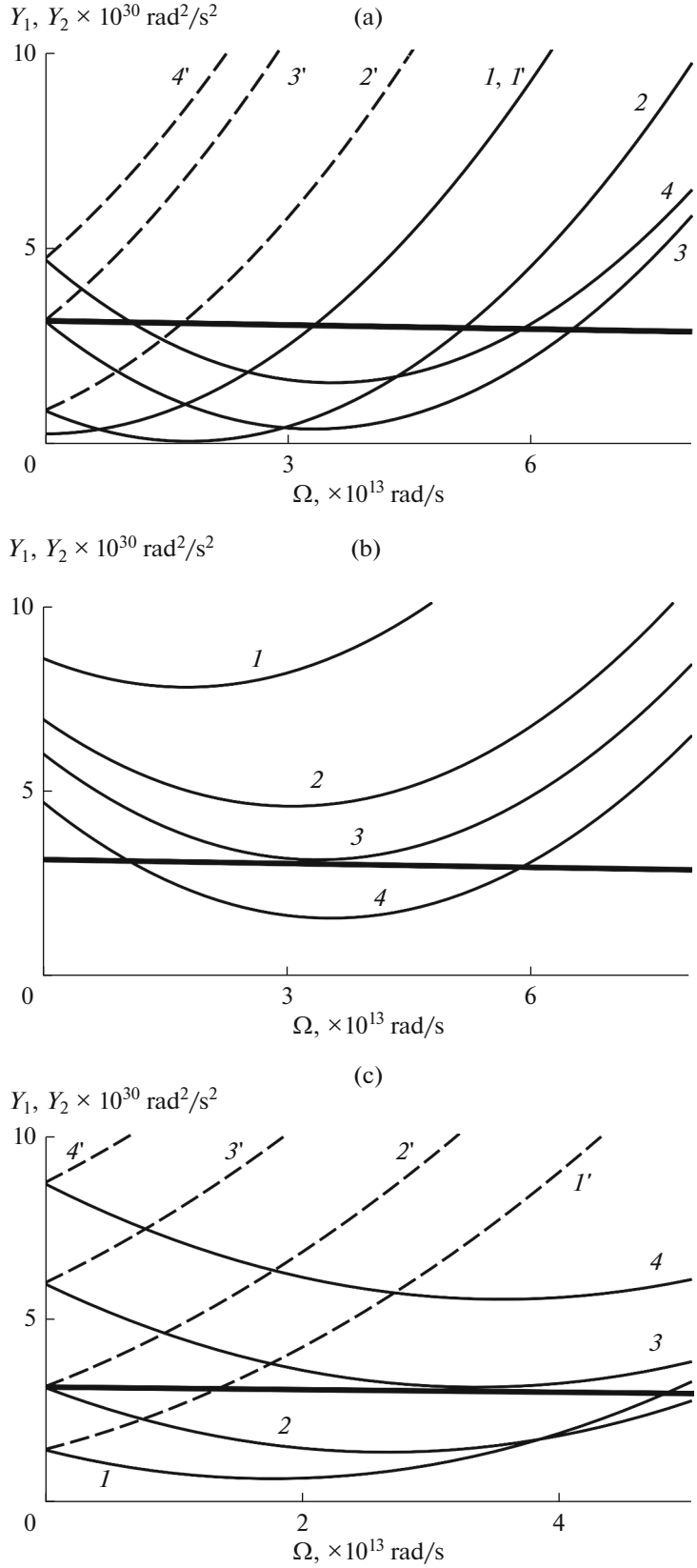

Fig. 3. Graphical solution of Eq. (8) with respect to the frequency of the PP: (a) at $d = 1.5$ μm (case $q > 0$), $\theta_1 = 0°$, 30°, 69° and 90° (*1–4*); (b) at $d = 1.5$ μm ($q < 0$), $\theta_1 = 30°$, 60°, 73° and 90° (*1–4*); (c) at at $d = 0.8$ μm, $\theta_1 = 0°$, 49°, 71° and 90° (*1–4*). Thick line, left-hand side of Y_1; thin line, right-hand side of Y_2; solid lines, case $\beta > 0$, dashed lines, case $\beta < 0$.

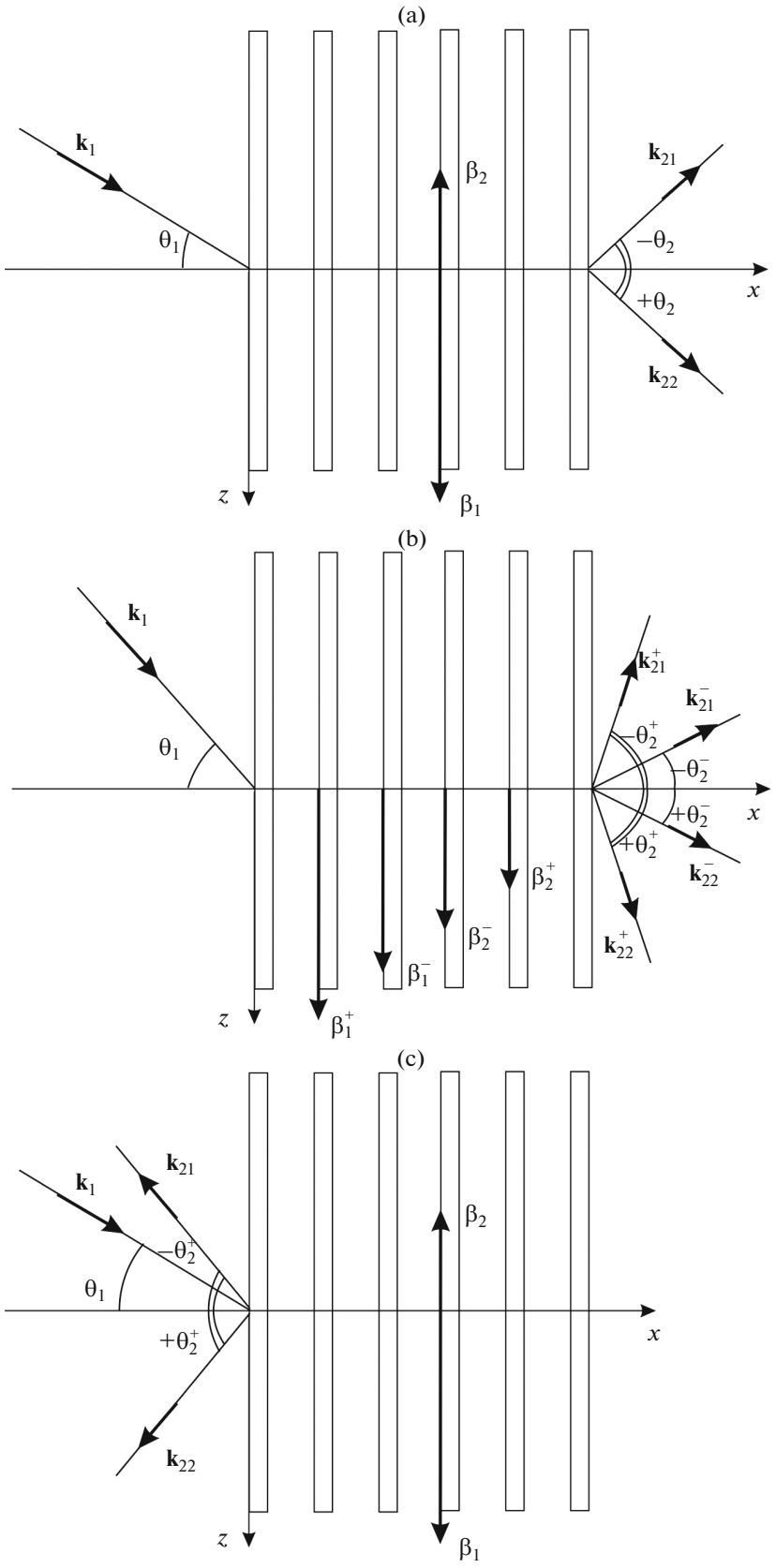

Fig. 4. Scheme of the wave vectors of the incident and diffracted laser beams, as well as PP excited in the CNT array: (a) $d > \lambda_1$, $\theta_1 < \theta_1^{cr} < \theta_1^{min}$; (b) $d > \lambda_1$, $\theta_1 > \theta_1^{min} > \theta_1^{cr}$; (c) $\lambda_1/2 < d < \lambda_1$, $\theta_1 < \theta_1^{cr} < \theta_1^{max}$.

be accute, not exceeding $\arccos(\lambda_1/d)$ in magnitude. At $\theta_1 = \theta_1^{min}$ only one additional diffracted beam is directed along axis x.

The results of the numerical solution of Eq. (8) for the case $\lambda_1/2 < d < \lambda_1$ are presented in Fig. 3c (for calculations, the values of the lattice period were chosen as $d = 0.8$ μm). Solutions with $q < 0$ in this case are absent. At $q > 0$, as in the previous case, there is a critical angle defined by the same formula (11) that has the same meaning; however, now its values fall in the range from 0° to 60°. There is another significant difference: there are no solutions if the angle of incidence exceeds the maximum allowable value:

$$\theta_1^{max} = \arccos(\lambda_1/d - 1). \quad (12)$$

In the conditions of Fig. 3c, the characteristic angles of incidence according to formulas (11) and (12) have the values $\theta_1^{cr} \approx 49°$ and $\theta_1^{max} \approx 71°$.

The diffraction angles in the case of $\lambda_1/2 < d < \lambda_1$ can only be obtuse; i.e., incident radiation is completely reflected from the structure. This is schematically shown in Fig. 4c for the angle of incidence from the interval $\theta_1 < \theta_1^{cr} < \theta_1^{max}$. At $\theta_1 = \theta_1^{max}$, the two roots merge into one at $\theta_2 = 180°$, i.e., there is one diffracted (reflected) beam and only one PP is excited in each nanotube. This situation seems to be optimal for increasing the efficiency of this structure used as an antenna in the THz range.

CONCLUSIONS

Laser-irradiated CNTs can be considered as generating antennas emitting in the THz radiation range and far infrared radiation range. As a result of successive reflections of the traveling surface wave from the ends of the plasmon waveguide formed by the nanotube, standing current and voltage waves are formed. For a given nanotube length of L there is a discrete set of frequencies for which the condition for the formation of standing waves $\beta(\Omega)L = m\pi$ (m is an integer). Note that in our case, resonances should be observed for wavelengths that in free space can significantly (by orders of magnitude) exceed the dimensions of the corresponding antenna, which is explained by the strong deceleration of the PPs.

Thus, it has been shown that near-infrared laser radiation can be used to efficiently generate THz and far-IR radiation under conditions of the two-beam laser irradiation of a non-periodic array of parallel CNTs and single-beam irradiation of an array of periodically located CNTs. It is important that the radiation frequency of a CNT array can be controlled by changing the angle of incidence of the laser radiation. Such an adjustment is required to fulfill the conditions of geometric resonance, as a result of which the efficiency of the radiating system can be sharply increased.

FUNDING

This work was supported by the Russian Foundation for Basic Research (project no. 18-29-19101) and by the Ministry of Science and Higher Education (project no. 0004-2019-0002).

REFERENCES

1. Lee, Y.S., *Principles of Terahertz Science and Technology,* New York: Springer, 2009.
2. Bratman, V.L., Litvak, A.G., and Suvorov, E.V., Mastering the terahertz domain: sources and applications, *Phys. Usp.,* 2011, vol. 54, no. 8, pp. 837–844.
3. Bugay, A.N. and Sazonov, S.V., The generation of terahertz radiation via optical rectification in the self-induced transparency regime, *Phys. Lett. A,* 2010, vol. 374, no. 8, pp. 1093–1096.
4. Fülöp, J.A., Pálfalvi, L., Klingebiel, S., Almási, G., Krausz, F., Karsch, S., and Hebling, J., Generation of sub-mJ terahertz pulses by optical rectification, *Opt. Lett.,* 2012, vol. 37, no. 4, pp. 557–559.
5. Nagai, M., Matsubara, E., and Ashida, M., High-efficiency terahertz pulse generation via optical rectification by suppressing stimulated Raman scattering process, *Opt. Express,* 2012, vol. 20, no. 6, pp. 6509–6514.
6. Sharma, S. and Vijay, A., Terahertz generation via laser coupling to anharmonic carbon nanotube array, *Phys. Plasmas,* 2018, vol. 25, no. 2, p. 023114.
7. Slepyan, G.Ya., Maksimenko, S.A., Lakhtakia, A., Yevtushenko, O.M., and Gusakov, A.V., Electrodynamics of carbon nanotubes: dynamic conductivity, impedance boundary conditions, and surface wave propagation, *Phys. Rev. B,* 1999, vol. 60, no. 24, p. 17136.
8. Sadykov, N.R. and Skorkin, N.A., Quantum approach to the description of amplification of radiation from an array of nanotubes, *Tech. Phys.,* 2013, vol. 58, no. 5, pp. 625–629.
9. Batrakov, K.G., Kibis, O.V., Kuzhir, P.P., da Costa, M.R., and Portnoi, M.E., Teraherz processes in carbon nanotubes, *J. Nanophoton.,* 2010, vol. 4, no. 1, p. 041665.
10. Batrakov, K.G., Maksimenko, S.A., Kuzhir, P.P., and Thomsen, C., Carbon nanotube as a Cherenkov-type light emitter and free electron laser, *Phys. Rev. B,* 2009, vol. 79, no. 12, p. 125408.
11. Shuba, M.V., Slepyan, G.Ya., Maksimenko, S.A., Thomsen, C., and Lakhtakia, A., Theory of multiwall carbon nanotubes as waveguides and antennas in the infrared and the visible regimes, *Phys. Rev. B,* 2009, vol. 79, no. 15, p. 155403.
12. Hanson, G.W., Fundamental transmitting properties of carbon nanotube antennas, *IEEE Trans. Antennas Propag.,* 2005, vol. 53, no. 11, pp. 3426–3435.
13. Hao, J. and Hanson, G.W., Electromagnetic scattering from finite-length metallic carbon nanotubes in the lower IR bands, *Phys. Rev. B,* 2006, vol. 74, no. 3, p. 035119.
14. Bulyarskii, S.V., Dudin, A.A., Orlov, A.P., Pavlov, A.A., and Leont'ev, V.L., Forced vibration of a carbon nano-

tube with emission currents in an electromagnetic field, *Tech. Phys.,* 2017, vol. 62, no. 11, pp. 1627–1630.

15. Chepurnov, A.S., Ionidi, V.Y., Kirsanov, M.A., Kitsyuk, E.P., Klenin, A.A., Kubankin, A.S., Oleinik, A.N., Pavlov, A.A., and Shchagin, A.V., Nanotubes based neutron generator for calibration of neutrino and dark matter detectors, *J. Phys.: Conf. Ser.,* 2017, vol. 934, no. 1, p. 012013.
16. Atdaev, A., Danilyuk, A.L., Labunov, V.A., Prishchepa, S.L., Pavlov, A.A., Basaev, A.S., and Shaman, Yu.P., Interaction of the electromagnetic radiation with the magnetofunctionalized CNT-nanocomposite in the subteraherz frequency range, *Izv. Vyssh. Uchebn. Zaved., Elektron.,* 2015, vol. 20, no. 4, pp. 357–364.
17. Kadochkin, A.S., Moiseev, S.G., Dadoenkova, Y.S., Svetukhin, V.V., and Zolotovskii, I.O., Surface plasmon polariton amplification in a single-walled carbon nanotube, *Opt. Express,* 2017, vol. 25, no. 22, pp. 27165–27171.
18. Wei, L. and Wang, Y.N., Electromagnetic wave propagation in single-wall carbon nanotubes, *Phys. Lett. A,* 2004, vol. 333, nos. 3–4, pp. 303–309.
19. Moradi, A., Surface plasmon-polariton modes of metallic single-walled carbon nanotubes, *Photon. Nanostruct.,* 2013, vol. 11, no. 1, pp. 85–88.
20. Moradi, A., Theory of carbon nanotubes as optical nano waveguides, *J. Electromagn. Anal. Appl.,* 2010, vol. 2, no. 12, pp. 672–676.
21. Martin-Moreno, L., Garcia de Abajo, F.J., and Garcia-Vidal, F.J., Ultraefficient coupling of a quantum emitter to the tunable guided plasmons of a carbon nanotube, *Phys. Rev. Lett.,* 2015, vol. 115, no. 17, p. 173601.
22. Attiya, A.M., Lower frequency limit of carbon nanotube antenna, *Prog. Electromagn. Res.,* 2009, vol. 94, pp. 419–433.
23. Nakanishi, T. and Ando, T., Optical response of finite-length carbon nanotubes, *J. Phys. Soc. Jpn.,* 2009, vol. 78, no. 11, p. 114708.
24. Sasaki, K., Murakami, Sh., and Yamamoto, H., Theory of intraband plasmons in doped carbon nanotubes: rolled surface-plasmons of graphene, *Appl. Phys. Lett.,* 2016, vol. 108, no. 16, p. 163109.
25. Miano, G. and Villone, F., An integral formulation for the electrodynamics of metallic carbon nanotubes based on a fluid model, *IEEE Trans. Antennas Propag.,* 2006, vol. 54, no. 10, pp. 2713–2724.